

参赛队员姓名：瞿任杰，戴昊辰，李宇晨

中学：上海市平和学校

省份：上海

国家/地区：中国

指导教师姓名：韩超群

指导教师单位：上海市平和学校

论文题目：Exploring the Thermodynamic
Properties of Rubber Band and Related
Refrigerator Design

Exploring the Thermodynamic Properties of Rubber Band and Related Refrigerator Design

By Qu RenJie, Li YuChen, Dai HaoChen

Abstract

This paper explores the refrigeration effect of a rubber band. When we stretch a section of rubber band, heat is released. When a rubber band experiences a thermodynamic cycle, a refrigerator can be achieved. The heat emission after stretching a rubber band is primarily a result of entropy change: the arrangement of polymers in the rubber band becomes more regular during stretching, resulting in a decrease of entropy.

Our goal is to develop a rubber-band refrigerator. To understanding the thermodynamic cycle of an ideal gas, it is necessary we to know the rubber band's equation of state first, i.e., the tension-elongation relation in a rubber band as a function of temperature. This equation of state is given in theory by the *Mooney-Rivlin (MR) model*.

We conducted experiments of isothermal stretch of rubber bands. The results fit well with the *MR model* and the coefficients of the model are also determined from experimental data. We also applied the Maxwell relation to deduce the entropy change during an isothermal stretch so that the heat exchange can be estimated. The *Gaussian statistical model* that describes the entropy change is also considered and compared to the experimental result.

Our paper describes important factors regarding refrigeration performance. This enables us to estimate the energy and heat exchange during a refrigeration cycle. For example, when stretching, heat emission occurs during maximum elongation; when releasing, heat absorption occurs after complete release. These processes can be combined to draw a reversible diagram, from which the theoretical *coefficient of performance (COP)* is determined.

We have also designed and created a real-world refrigerator prototype. It successfully reduced the temperature of 100ml of machine oil by 0.7°C in 3 minutes.

Keywords: rubber band, refrigerator, *Elastocaloric effect*, elastic mechanics, *Gough-Joule effect*, Gaussian statistical model, entropy change, strain energy, hysteresis

Faith Statement

丘成桐中学科学奖-学术诚信声明

本参赛团队郑重声明：

1. 参赛团队提交的参赛队员和指导老师信息完整且属实无误。
2. 所提交的研究报告是在指导老师指导下进行的研究工作和取得的研究成果。
3. 尽本团队所知，除文中加以标注和致谢中所罗列的内容外，研究中不包含其他人已经发表或撰写过的研究成果，不存在代写或其他违规行为。

以上，若有不实之处，本人愿意承担一切相关责任，并服从丘成桐中学科学奖组织委员会的裁决。

参赛学生（签字）：

戴星辰, 瞿任杰, 李承蒙

本校指导老师（签字）：

韩超峰

学校名称（加盖学校或教务处公章）：

外校指导老师（签字）：

单位名称（加盖单位公章）：

2022年9月19日

Table of Contents

I. Introduction	5
II. Mechanical and thermodynamic properties of elastomer	6
2.1. Elastomer's tension-elongation relation: the Mooney-Rivlin model	6
2.2. Thermodynamic properties: entropy change during stretching by "Gaussian" statistical model	7
III. Experiments	9
3.1. Measuring the rubber band's tension during isothermal stretching and comparison with MR Model	9
3.2. Heat absorption (discharge) during isothermal stretching and contraction	13
IV. Rubber-band-based refrigerator	15
4.1. Refrigerating cycle of rubber band	15
4.2. Rubber band refrigerator prototype	16
V. Conclusion and outlook	18
VI. Bibliography	20
VII. Thanks	21
VIII. Team member's information	22
IX. Experimental location and time	23
X. Appendix	24
X.1. Explanation and derivation of Gaussian Model	24
X.2. Tension change in response to temperature increase	26
X.3. Fatigue effect	28
X.4. Preliminary experiment and compensation function	28
X.5. Hysteresis	30

I. Introduction

When stretching a rubber band, the its absolute temperature will increase with the increasing strain*¹ as well as tension. Such correlation of elastomeric material was first found as the *Gough-Joule effect* in the 19th century¹.

In the following years, there were several other scientists explained the thermodynamics of the stretching rubber band²⁻³ on the microscopic scale. It was discovered that such *electrocaloric effect*⁴ of elastomeric material is governed primarily by changes in entropy: when the rubber band is in the relaxed state, the two terminals of polymers are randomly located, exhibit the most chaotic state, and have maximum configurational entropy. When the rubber band is elongated, all the polymers within would also be stretched, with the terminals fixed at more separated points and crystallization structure. Consequently, the Boltzmann entropy would decrease.

In the past few decades, due to the destructive effect of Freon on the atmosphere in conventional refrigeration machines and the need for more environmentally friendly methods of refrigeration, the study of the thermal effects of elastomers had regained importance. In the meantime, scientists had successfully tested and measured the heat gain of elastomers in different conditions of stretching⁵⁻⁸: spherical expanded, linear stretched twisted, and super-coiled.

In this paper, further thermodynamics and mechanics of rubber band related to the *elastocaloric* effect of elastomer was investigated, and some existing models have been evaluated.

For the mechanical properties of elastomer, the *Mooney-Rivlin model*⁷ (*MR model*) was used to fit the data of stress-strain response. Since the coefficients of the MR model is temperature determined, the tension in a rubber band as a function of temperature and strain can be determined through experimental approaches.

For the energy associated with entropy change of elastomer, inspired by the method using in "*Exploring the thermodynamics of a rubber band*"⁹, we've "measured" and calculated the entropy change by using a Maxwell relation for an isothermal stretch. Then, we compared the result calculated through maxwell relation with the entropy change predicted by the *Gaussian model*³ and further analyzed the result.

Furthermore, we've compared the MR model with the Gaussian model and deduced a more quantitative conclusion about the actual heat absorption (release) during the stretching of elastomer which could be an effective prediction for our later refrigerating process.

Finally, our real-world refrigerator had been designed and created. Its performance in a 3-minute-refrigerating was tested. It successfully reduced the temperature of 100ml of machine oil by 0.7°C. We have also discussed the coefficient of performance (COP) for the rubber refrigerator and compared it to the theoretical COP. Thus, the actual cooling effect and feasibility of a small rubber refrigerator could be discussed and evaluated.

*¹ Relationship between strain e , stretch λ and elongation Δl :

$$\lambda = e + 100\% = \frac{\Delta l + l_0}{l_0}$$

II. Mechanical and Thermodynamical Properties of Elastomer

2.1 Elastomer's tension-elongation relation: the Mooney-Rivlin model

In general, the mechanics of rubber band was often described by Hooke's Law and Young's Modulus^{10,11}, which states the tension is proportional to the elongation. However, to accurately describe the actual tension-elongation relationship in an elastomer, further physical properties of the rubber band and the continuum mechanics treatment for considering the nonlinearity pattern within the elastomer mechanism should be investigated.

One of the basic properties we shall consider before analyzing the mechanism is the compressibility of an elastomer. A general method to describe the compressibility of a material is the Poisson ratio " ν " defined by:

$$\frac{dV}{dL} = (1 - 2\nu) \frac{V}{L}, \quad 'V' \text{ the volume and } L \text{ the length} \dots \dots \dots (1)$$

In "*limits to Poisson's ratio in isotropic materials*"¹², P.H. Mott et.al measured the Poisson's ratio of isotropic rubber bands at Room Temperature which is 0.4999. Similar results that the Poisson's ratio of 2.2mm *Natural Rubber (NR)* fibers was close to 0.5 (between 0.5 and 0.48) up to 500% Strain was achieved by Run Wang et.al⁵ through taking photos by high-speed cameras and observing the deformation pattern of *NR* fibers under high strain. Therefore, we could conclude that the rubber band is an incompressible solid, which means the volume of the rubber band would remain the same for all the conditions in our experiments.

Then, to further discuss the tension-stretch patterns of elastomer, an accurate expression of tension must be determined. Typically, the strain energy density of a stretched object can be calculated with young's modulus. However, traditional Young's modulus is not available for rubber bands since the deformation of it is normally on a large scale (0%~200% strain in our experiment).

In 1940, for elastomer with *Superelasticity*^{*2} such as *Natural Rubber (NR) fibers*, M. Mooney derived the corresponding function of strain energy density with principal stretch state $\lambda = \frac{\Delta l + l}{l}$ along three principal directions $(\lambda_1, \lambda_2, \lambda_3)$, based on continuum mechanics in elastic mechanics⁸, known as MR model:

$$W_{MN} = C_{10}(I_1 - 3) + C_{01}(I_2 - 3) \dots \dots \dots (2)$$

$$\text{where } I_1 = \lambda_1^2 + \lambda_2^2 + \lambda_3^2, \quad I_2 = \lambda_1^2 \lambda_2^2 + \lambda_2^2 \lambda_3^2 + \lambda_3^2 \lambda_1^2$$

To get those parameters, the expression of the tension should be deduced since the value of strain energy density can't be measured directly. For the uniaxial stretch in our experiment, a simplified function of

^{*2} A combination of a series of properties for ideal elastomer defined by M. Mooney in the paper "*A Theory of Large Elastic Deformation*" which satisfy the following three properties: 1. The material is isotropic in the undeformed state and at right angles to the deformed state. 2. The deformations are isometric 3. The traction in simple shear in any isotropic plane is proportional to the shear.

tension could be derived by doing the partial differential of the strain energy density relative to the elongation due to the symmetry and incompressibility of the NR fibers that we used:

$$\text{Let } \lambda_1 = \lambda = \frac{\Delta l + l}{l}, \quad \text{then: } \lambda_2 = \lambda_3 = \frac{1}{\sqrt{\lambda}}$$

$$\tau = \left(\frac{\partial F}{\partial l} \right)_T = V_0 \times \left(\frac{\partial W_{den}}{\partial l} \right)_T$$

$$\frac{\partial W_{den}}{\partial l} = \frac{\partial \lambda}{\partial l} \left[\frac{\partial W_{den}}{\partial I_1} \frac{\partial I_1}{\partial \lambda} + \frac{\partial W_{den}}{\partial I_2} \frac{\partial I_2}{\partial \lambda} \right] = \frac{1}{l_0} \left[C_{10} \left(2\lambda - \frac{2}{\lambda^2} \right) + C_{01} \left(2 - \frac{2}{\lambda^3} \right) \right]$$

$$\tau = V_0 \frac{\partial W_{den}}{\partial l} = 2S_0 \left(C_{10} + C_{01} \frac{1}{\lambda} \right) \left(\lambda - \frac{1}{\lambda^2} \right) \dots \dots \dots (3)$$

Eq. 3 is the tension-elongation relation given by the MR model. Furthermore, compared with the form of the model listed by Flory⁸ and Erman which has the same prediction trend and performance as the MR model, we could assume that the coefficients in the MR model should be functions of temperature. (Similar conclusion could be arrived at by comparing it with our experimental data or the result of the Gaussian model.) i.e.

$$C_{10} = C_{10}'(T), \quad C_{01} = C_{01}'(T)$$

Therefore, the MR model could be further modified by fitting the tension in a rubber band as a function of temperature and elongation*³ to Eq.3.

2.2 Thermodynamic properties: entropy change during stretching by the “Gaussian” statistical model

Although the Gough-Joule effect seemed to disobey people’s common sense, it is quite easy to understand if we consider the entropy change through the stretching process. As mentioned in the introduction part, while people stretch the rubber band, the configurational entropy of the elastomer actually decreases. Such entropy decrease leads to heat discharge that consumes the energy input by external work, causing a temperature increase of value “ΔT”. Since the change in temperature of an elastomer is normally very small compare to its original temperature (ΔT << T₀), the increase of temperature during the stretching of elastomer is approximated as:

$$\Delta T = \frac{\Delta Q_{config}}{C_{total}} \approx \frac{T_0 \Delta S}{C_{total}}, \text{ where } C \text{ is the total heat capacity}$$

Therefore, it is useful to derive an analytic expression of the Boltzmann entropy change for the rubber band during the stretching process. In order to further investigate the Gough-Joule effect quantitatively, the best approach to derive the entropy change model for an elastomer would be to consider the microscopic changes of the polymers of an elastomer in statistical method.

Still, a list of chemical and molecular properties of the microscopic construction should be mentioned as the precondition before deriving the analytic expression of entropy change. Basically, a natural rubber molecule is made by the polymerization of isoprene (C₅H₈)_n and it is known as cis-1,4-polyisoprene with an average molecular weight of 100,000 to 1,000,000¹³. The natural rubber polymers are formed as

*³ Further investigation can be seen in Appendix 2

tangled long chains since they consisted of loosely jointed monomers of C_5H_8 . According to the molecular degree and the monomers formula, we could calculate its degree of polymerization:

$$DP = \frac{M}{M_0} = \frac{M(poly)}{M(C_5H_8)} \approx 1500 \sim 15000 \dots \dots \dots (4)$$

Since the link between adjacent monomers could freely rotate in a given planar, such a high degree of polymerization allows the links between the monomers to be considered almost equivalently as random orientations and shows such Gaussian property in the distribution of probability density, which is of great benefit for the derivation of the following entropy change model for the rubber molecule.

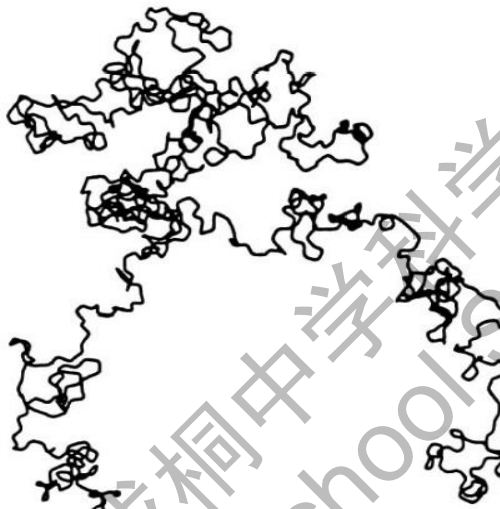


Figure 2-1: Form of 1000-link polymethylene chain (randomly orientated) in statistical theory³

In 1943, based on the aforementioned properties of rubber molecule and several other assumptions*⁴, Treloar, Flory and Rehner, and James and Guth respectively derived the entropy change in NR band based on the distribution of the end-to-end polymer length*⁵.

$$\Delta S_{total \text{ per Unit Volume}} = -\frac{1}{2} Nk(\lambda_1^2 + \lambda_2^2 + \lambda_3^2 - 3), \quad N \text{ number density} \dots \dots \dots (5)$$

In conventional theory¹⁴, since the internal energy change at fixed temperature was often neglected as 0, the occurrence of tension in the rubber band was simply attributed to the loss of energy associated with the configurational energy. However, both in the MR model and several other experiments⁹, the existence of change of internal energy relative to the change of length at fixed temperature was verified and was proven to contribute to the generation of tension. Therefore, in the later section, the performance of this model would be discussed and evaluated. It will be compared with the MR model, as well as to entropy change based on Maxwell relation as described below.

*⁴ Five assumptions that were stated by Treloar as the necessary assumption for the Gaussian statistical model:1. Homogenous 2. Identity 3. Incompressibility 4. Affine deformation 5. Total entropy of network is the sum of individuals'
 *⁵ Rigorous proof of Gaussian model will be shown in Appendix 1

III. Experiments

3.1 Measuring the rubber band's tension during isothermal stretching and comparison with MR Model

Experiment Introduction

The experimental setup of isothermal stretch is in Fig.3-1. In the experiment, a 1mm×2mm rubber band with original length l_0 *⁶=18cm was stretched and contracted with different levels of strain from 0% to 89.9% at temperature from 8.5% to 67.2%, and its elongation value and the corresponding tension of the rubber band were measured to fit the tension-relationship model given by MR model. During the whole stretching process, the rubber band was immersed in the water so that the change of its temperature is negligible. To study the tension of elastomer at different temperatures and lengths, the temperature of the water in an acrylic tube was controlled by adding boiled water and ice, while the large heat capacity of a tube of water ensured the temperature of the liquid remained almost unchanged before and after the stretching process

Since the rubber band is immersed in water, it is not convenient to measure the elongation by manually reading the ruler hanging outside of the tube, (and it is not conducive to our analysis of the continuous stretching process by measuring only discrete values.) Alternatively, the video analysis techniques conducted through Logger Pro 3.14 and Tracker were used through recording the stretching process and extension condition of the rubber band at a horizontal view (adjust through external spirit level), then used the scale bar and the magnification of the video image to measure the length elongation for the rubber band. At the same time, since the rubber band itself needs extra length to be fixed on the thread hook and hung on the force gauge, we cannot accurately calculate the overall length of the rubber band stretch. However, it is worth noting that the stretch of each segment of the rubber band and the tension of each segment should be the same due to the rubber's isotropic and affine deformation nature. Therefore, we obtained the elongation of the real rubber band by measuring its elongation in the camera image and multiplying it by the scale bar.

For the tension measurement, since the maximum tension of the rubber band was merely above 0.25N, which is only slightly larger than the minimum scale value of a normal dynamometer, we can't use the normal dynamometer to measure the tension of the rubber band*⁷. As an alternative, we've used a *high precision kitchen electronic scale* with a minimum scale of 0.1g to measure the tension of the rubber band, which is the difference between the reading of mass times the gravitational acceleration. Such high-precision devices enabled us both to measure the small tension of the rubber band effectively and with high precision. Considering the response time and the reading changing threshold of the digital scale, the measurement uncertainty is taken as ±3g considering the fluctuations in the measured value.

*⁶ The distance between the black dot and the thread hook at relaxed state, which explained later

*⁷ We have tried many ways to increase the tension of the rubber band: such as replacing the diameter of the rubber band, changing the rubber band specifications, the rubber band folded around more than one turn, etc. For the first two, the only kind large Natural Rubber band available to buy in online or offline shops are those round rubber hoses with the middle hollowed. These rubber hoses are usually manufactured after its own bending and a certain amount of strain, so it is impossible to determine its original length at relaxed state. And for the last method, we found that even only folded once, due to the large friction between rubber surfaces, the results are affected.

Experiment Procedure

1. Tap the threaded hook into the rubber stopper.
2. Tie one end of a long rubber band on the hook, keep the band straight and relaxed, and leave a mark 18cm from the knot.
3. Insert the stopper into one end of the transparent acrylic tube hard to make sure that the opening is completely sealed.
4. Leave a mark 18cm from the knot on the outer surface of the tube and leave one every 2cm above along the whole tube.
5. Use ice to cool water down to below 10°C and fill the tube with cold water.
6. Put the tube on the electric scale and set zero the device.
7. Wait for 2 minutes to make sure that the temperature of the rubber band is the same as the water. Then, use the electric thermometer to measure the temperature of the water.
8. Start stretching the rubber band slowly upwards. Meanwhile, use a cell phone to record the position of the mark on the rubber band and tube and use another to record the reading of the electric scale.
9. Repeat steps 5~8 with water at temperatures from 10°C to 70°C .

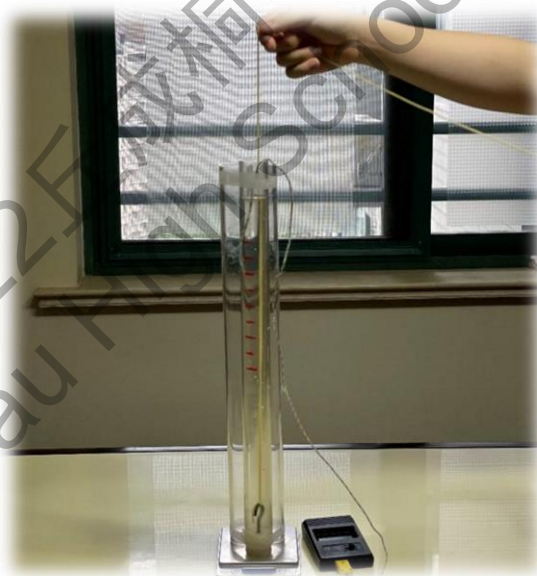


Figure 3-1: Setup for isothermal stretch experiment

During the stretching process of the rubber band, as the experimenter was standing on the side of the acrylic tube, there wasn't almost any left and right movement in the experimenter's view plane. However, such inclination of the stretched rubber band will occur in the view plane of the camera and the measured tension and elongation will both be inaccurate since the measured tension was only the vertical component of the actual tension applied on the rubber band. Furthermore, since the rubber band was stretched several times to evaluate the performance of the MR model at different temperatures, the fatigue

effect of the rubber band should also be taken into account (as described in Appendix 1). Therefore, preprocessing of the raw data before fitting and evaluating the MR model is necessary for this experiment.

First, according to the coordinates of the two endpoints of the rubber band in the video, we can calculate the precise elongation value of the rubber band through the following equation:

$$\Delta L = \sqrt{\Delta x^2 + (l_0 + \Delta y)^2} - l_0 = (l_0 + \Delta y) \left(1 + \frac{\Delta x^2}{(l_0 + \Delta y)^2} \right)^{\frac{1}{2}} - (l_0 + \Delta y) + \Delta y$$

Because $\Delta x^2 \ll (l_0 + \Delta y)^2$, through binomial expansion, a simplified would be given:

$$\Delta L \approx (l_0 + \Delta y) \left(1 + \frac{\Delta x^2}{2(l_0 + \Delta y)^2} \right) - (l_0 + \Delta y) + \Delta y = \frac{\Delta x^2}{2(l_0 + \Delta y)} + \Delta y \dots \dots \dots (6)$$

Secondly, since the vertical component of the tension is balanced with the normal reaction force and the gravitational force, the actual tension and the change of reading on the digital scales should follow the equation below:

$$\cos(\theta) m_{reading} g = \tau' \cos(\theta) = \tau,$$

τ' the measured value of tension,

θ is the included angle between instantaneous tension direction and gravitational force direction

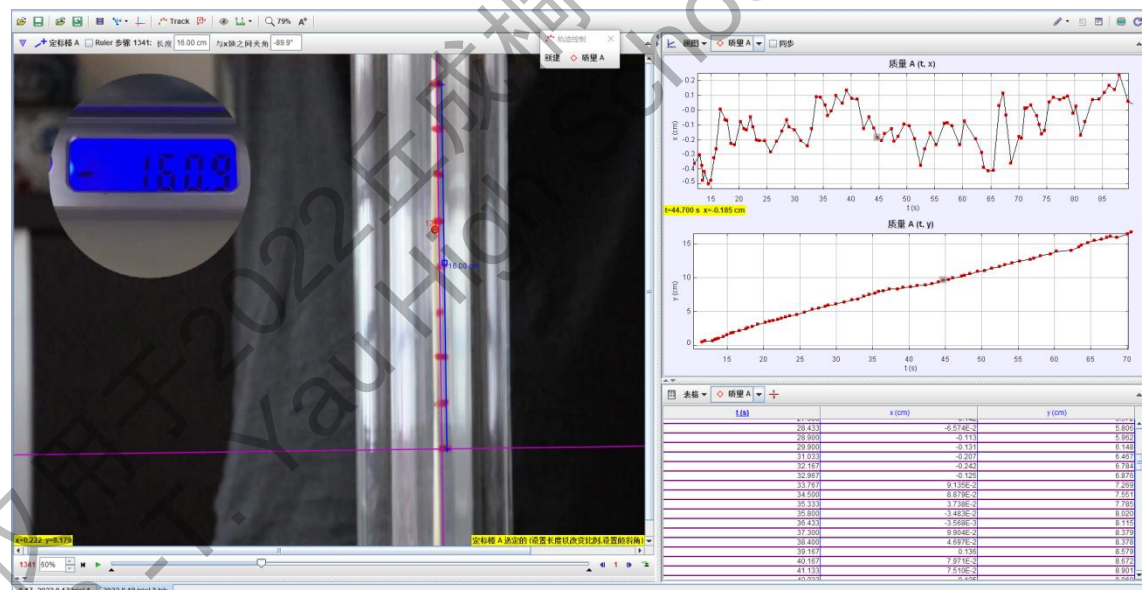


Figure 3-2: Video analysis of instantaneous elongation of elastomer by Tracker (with corresponding tension reading of digital scale shown on the left of the image)

MR model fit on tension and evaluation

The experimental results of tension-elongation relation at 8.5°C, 49.6°C, and 67.2°C are shown in Fig.3-3. The parameters of the rubber band (including initial length 18cm and S0-1mm×2mm, etc.) were brought into the MR model for fitting. The lost function we used for evaluation and curve-fitting is the Least-Mean-Square-Error (LMSE), and the following conclusions were obtained:

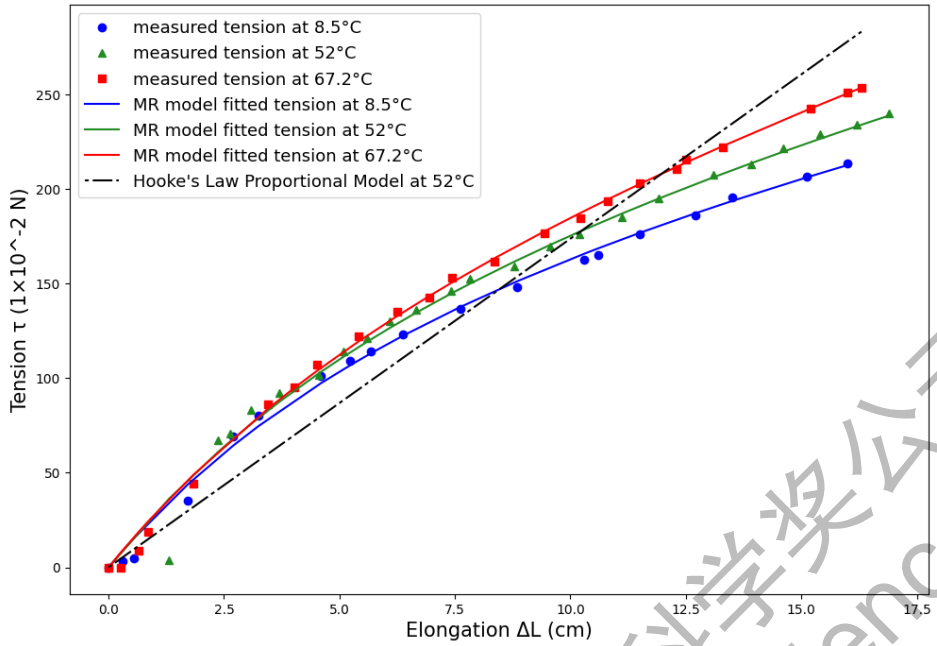


Figure 3-3: Tension vs. elongation. The colorful curves are fits with the MR model, while the black line fits with Hooke's Law.

In general, compared with the traditional Hooke's Law Linear Fit (i.e., the black line in the figure), the MR model was able to fit the value of Rubber band tension smoothly and accurately for a total of 68 data points. The coefficient of correlation of the MR model reaches 0.996 in average, and its Root-Mean-Square-Error (RMSE) value is merely 34.7% that of Hooke's Law. Therefore, it can be shown that the MR model is a good fit for the stretching of the model rubber bands used in this experiment.

Meanwhile, for low strain, we did not find a clear positive correlation between tension of the rubber band and temperature suggested by the Gough-Joule effect. This phenomenon is consistent with the expectation we concluded in the fatigue experiment (Appendix 3) that the value of elastomer's tension was more random and less correlated with stretch and temperature at a low stretch. Moreover, combined with the present experimental data, it can be concluded that under the low elongation (0~4cm, 20% strain), the performance of tension and temperature even shows a negative correlation, which starkly against the expectation of Gough-Joule effect. Similar phenomenon was observed by R. L. Anthony et. al¹⁵ as well in the case of high tension, large diameter NR fibers with strains less than 10%.

Strain energy data fit and MR model evaluation

Since the MR model has a very high performance in fitting the data of tension between 0~100% strain, the model in the form of a strain energy function ought to be evaluated to prevent overfitting in tension form.

According to the definition of strain energy F , its relation with the actual tension of the rubber band could be easily deduced:

$$\frac{\partial W_{density}}{\partial l} = \left(\frac{dF_{total}}{V_0 dl} \right)_T = \left(\frac{\tau}{V_0} \right)_T, \quad \Delta F = V_0 \Delta W = \int_{l_i}^{l_f} (\tau dl)_T \dots \dots \dots (7)$$

Based on the densely taken points of the previous experimental data, the RHS of equation (7) (the integral part) can be obtained directly by summing the area of the trapezoid enclosed by the adjacent tension data

points and the coordinate axes in Fig.3-3. At this point, given the conditions of elongation, we can directly compare the fit results of the actual strain energy change and the MR model energy change by using the coefficients in the MR model that we obtained in the previous tension fit.

$$C_{10} = B \frac{A}{2S_0}, C_{01} = C \frac{A}{2S_0}, \quad A, B, C \text{ coefficients fit by the logger pro, } S_0 \text{ section area of relaxed state}$$

Unit: 10 ⁻² N·cm ⁻²	C_{10}	C_{01}	Parameters	$W_{MNtotal}$	W_{actual}
High (67.2°C)	3204.87	1302.65	$\lambda = 1.8889$	23.73 N·cm	23.62 N·cm
Mid (49.6°C)	2484.95	2102.68	$I_1 = 4.6267$	22.56 N·cm	22.29 N·cm
Low (8.5°C)	2089.59	2295.54	$I_2 = 4.0581$ $V = 3.6 \times 10^{-1} cm^3$	20.98 N·cm	20.85 N·cm

Table 3-1: Parameters of the rubber band, fitting total strain energy of MR model and actual strain energy measured through integration at maximum strain

According to the data table above, we could barely conclude that: In the case of strain 90% or less, the MR model fits the tension and strain energy density with excellent performance (the error of predicted Strain energy and actual work down is within 2%).

In conclusion, we've both evaluated the MR model in tension form and the strain energy form respectively. In both cases, the MR model showed excellent performance, which provided us with data support for the subsequent use of the MR model directly instead of the measured data as the fitting function for the tension of the rubber band.

3.2. Heat absorption (discharge) during isothermal stretching and contraction

Finally, entropy-change-related thermodynamics of the stretching process and the performance of the Gaussian model were investigated. However, since it is impossible for us to measure the entropy change directly, method that calculate the change of entropy indirectly should be applied. We used a Maxwell relation to represent the change of entropy by:

$$\left(\frac{\partial \tau}{\partial T}\right)_l = -\left(\frac{\partial S}{\partial l}\right)_T$$

$$\Delta S = \int \left(\frac{\partial S}{\partial l}\right)_T dl = \int -\left(\frac{\partial \tau}{\partial T}\right)_l dl, \text{ where } T = T_0 \text{ is fixed (8)}$$

According to Eq. 8, the change of entropy can be calculated based on the tension-temperature data that we obtained in the former experiment. However, for the partial differential value of tension relative to temperature change, the former proportional model seemed can't perfectly fit the tension-temperature curve in the low strain region. Therefore, the improved linear model that we used as the comparison function was used to match the average value of $(\partial \tau / \partial T)_l$:

$$\left(\frac{\partial \tau}{\partial T}\right)_l = \left(\frac{\partial(\alpha T + \beta)}{\partial T}\right)_l = \alpha_{bestfit}(l), \quad \Delta S(l) = \int \alpha_{bestfit}(l) dl \quad \dots \dots (9)$$

For $\alpha_{bestfit}(l)$, we've used *Vscode Python* to find the best-fit-linear function under a fixed strain by the LMSE algorithm and use the coefficients of the first order term of this function as $\alpha_{bestfit}$. Then, we set the fitting step length of this $\alpha_{bestfit}$ to 0.0001cm and fitted the values of entropy change under each elongation by the idea of micro-element summation. Finally, we compare the fitted Gaussian model under the LMSE algorithm with our previous values of entropy change by Maxwell relation and summing of the infinitesimal, and we draw the following conclusions.

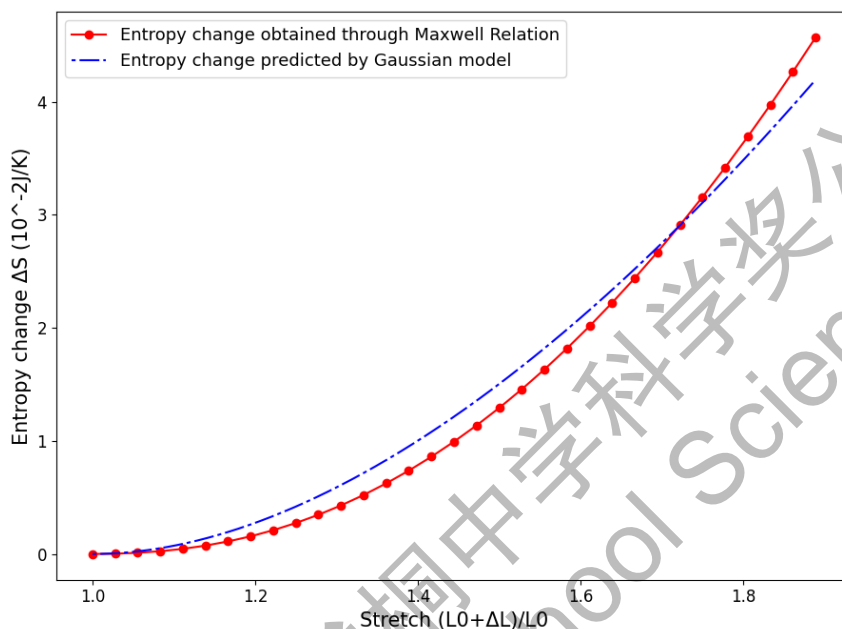


Figure 3-9: Entropy change calculate through Maxwell relation and Gaussian Model curve fit

In general, from the figure above, we can find out that the Gaussian model has a very high performance in regions below 100% elongation (correlation 0.9723) when we predict the entropy change of the rubber band.

Secondly, since we've noticed that the entropy change is independent of the temperature during stretching, we've calculated the actual maximum entropy change of this experiment through the Maxwell relation and give the expression of heat gain of the rubber band due to the energy loss related to configurational energy:

$$Q_{gain}(T) = T\Delta S_{config} = T \int \left(\frac{\partial \tau}{\partial T}\right)_l dl \approx 4.570T \times \frac{10^{-2}J}{K} \dots \dots \dots (10)$$

However, when comparing the heat gain with the increases in strain energy, it was found the heat gain is less than the strain energy increases. Furthermore, compared with the strain energy density expression and heat gain expression (entropy change times temperature) given by Gaussian model, we notice that the C_{10} term of MR model has the exact same form with the Gaussian model. Therefore, we decided to calculate the ratio between heat gain (according to the loss of entropy) and the change of total strain energy, and we obtained the following results:

$$\gamma(T, \Delta l) = \frac{T\Delta S(T, \Delta l)}{\Delta W((T, \Delta l))}, \text{ where } T \text{ is fixed } \dots \dots (11)$$

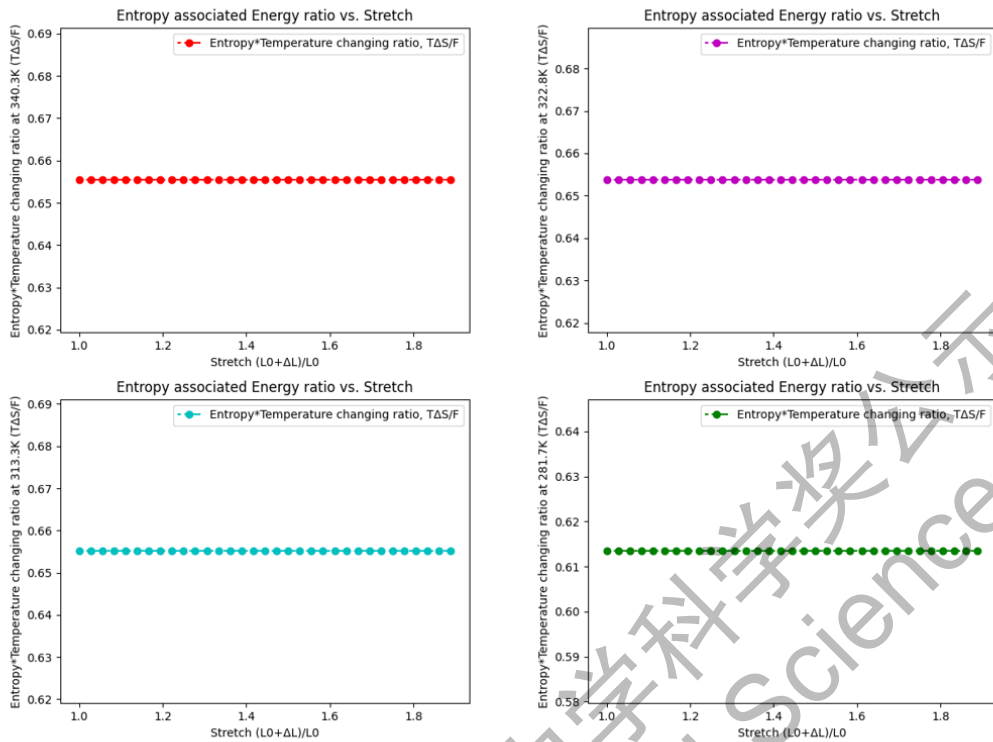


Figure 3-10~13: the value of $\gamma(T, \Delta l)$ vs. elongation at 340.3K, 322.8K, 313.3K, 281.7K these four temperature intervals respectively

Unit: 10 ⁻² N·cm ⁻²	Actual Work down (10 ⁻² J)	Heat gain (10 ⁻² J)	γ_{ratio}
High (67.2°C)	23.62	15.55	65.8%
Mid (49.6°C)	22.29	14.74	66.1%
Mid (40.1°C)	21.78	14.31	65.7%
Low (8.5°C)	20.85	12.97	62.2%

Table 3-2: the value of γ_{ratio} at maximum strain at four temperature intervals respectively

According to the above graph and table, we can find that the ratio of rubber band heat gain to strain energy change remains almost constant ($\pm 0.5\%$) during the stretching process at the same temperature. In addition, the ratio of heat gain and strain energy change is almost constant at $65\% \pm 3\%$ in four temperature intervals from 8.5 to 67.2°C. In summary, we can infer that the ratio of the rubber band's heat gain and strain energy in our experiment is about 65% in the region where the maximum elongation is below 100%. This conclusion can be used in the subsequent efficiency calculation of the refrigerator.

IV. Rubber band-based refrigerator

4.1 Refrigerating cycle of rubber band

With all the results we gained in previous experiments, we now try to construct a refrigerating cycle based on the rubber band to see how it performs. We first need to derive the maximum efficiency that can be reached by such a machine. To this end, we need to set a few basic assumptions:

1. Hysteresis effect doesn't occur in each cycle
2. Heat conduction doesn't require any time
3. All the heat and cooling effects were hundred percent used.

In addition, we want to make the cycle we design physically achievable, which means it is solely based on the stretching, contraction, and translational motion of the rubber band between the hot and cold reservoir. Based on these conditions, we constructed the following ideal cycle and calculated its COP:

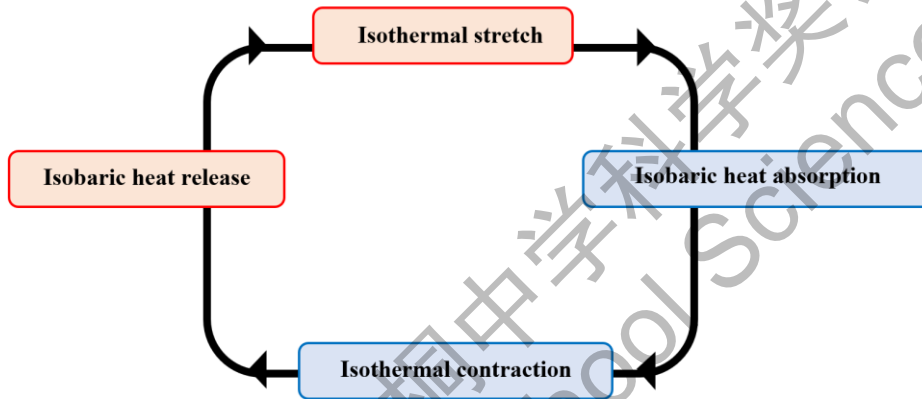


Figure 4-1: Refrigerating cycle

Part 1: Heat lost in hot reservoir:

$$Q_{lost} = \gamma \Delta W_h = \gamma (C_{10h}(I_1 - 3) + C_{01h}(I_2 - 3))$$

Part 2: Heat lost in cold reservoir:

$$Q_{lost} = C_{Rub} \Delta T = C_{Rub}(T_h - T_c)$$

Part 3: Heat gain in cold reservoir:

$$Q_{gain} = \gamma \Delta W_l = \gamma (C_{10l}(I_1 - 3) + C_{01l}(I_2 - 3))$$

Part 4: Heat gain in hot reservoir:

$$Q_{gain} = C_{Rub} \Delta T = C_{Rub}(T_h - T_c)$$

Then we define the *coefficient of performance (COP)* of the refrigerator:

$$COP = \frac{Q_{low\ lost}}{W} = \frac{(\gamma(C_{10l}(I_1 - 3) + C_{01l}(I_2 - 3)) - C_{Rub}(T_h - T_c))}{\Delta C_{10}(I_1 - 3) + \Delta C_{01}(I_2 - 3)}$$

4.2 Rubber band refrigerator prototype

After deriving the theoretical thermodynamic cycle of a refrigerator based on the rubber band, we built a real machine to verify whether rubber can be the working medium for refrigeration. Given our limited

budget, we didn't aim to build a machine that has real applications. Instead, we want to use the accessible materials to design a prototype that can is just capable of causing a measurable temperature drop. Here we present the refrigeration machine we designed.

First, since the mechanism of rubber band refrigeration requires the physical movement of the rubber band between the hot reservoir and the cold reservoir, it is impossible to seal the substance being cooled from the air. Thus, we choose to cool liquid instead of gas so that convection won't be a problem.

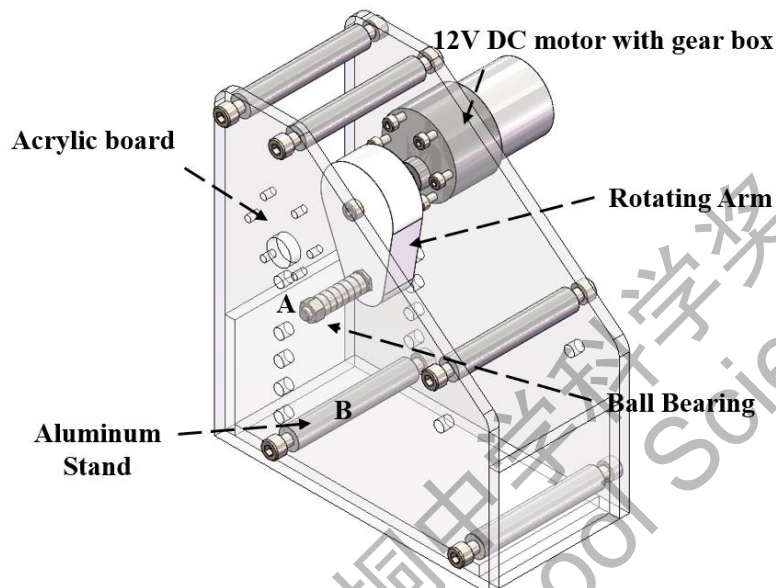


Figure 4-2: CAD Model of Rubber band Refrigerator

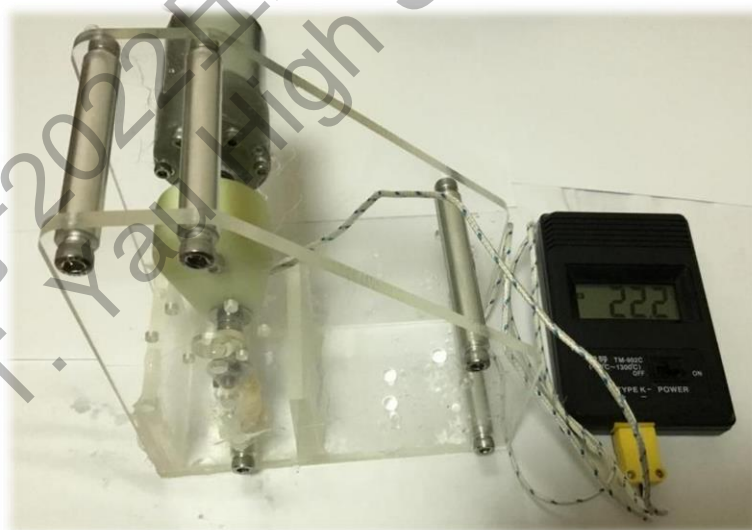


Figure 4-3: Real prototype refrigerator

Figure 4-2 is the computer-rendered picture for the design of our prototype. The real prototype refrigerator is shown in Fig.4-3.

The frame of this machine is made up of five acrylic boards which are designed by ourselves and laser-cut in a local machine shop. The three rectangular boards on the bottom are sealed with each other to be

small container for holding liquid. Five aluminum stands tapped with M5 thread are added to provide sufficient structural strength to take the tension of rubber bands. A 12V DC motor is the source of power, and a gearbox is mounted on it to increase torque to stretch rubber bands. The motor directly powers a 3D-printed rotating arm with a screw and ball bearings on its end. One end of the rubber band is fixed on the bearings at point A, and the other is fixed on the aluminum stand at point B. Thus, as the motor turns the arm, the distance between A and B changes, and the rubber band is stretched and released continuously.

Figure 4-4 (a) and (b) show different states of the machine in one of its complete cycles. The white part represents the air while the blue part represents liquid to be cooled. When point A moves away from point B, the motor does work on the rubber band and part of this increment of energy becomes heat. This is similar to the adiabatic stretching and isometric heat loss in Sec. 4.1. Since a longer section of rubber bands stay in the air, heat transfers from the rubber bands mainly to the air instead of liquid. Reversely, as the rubber bands get relaxed, it absorbs most energy from the liquid instead of the air, which corresponds to the adiabatic unloading and isometric heat gain process.

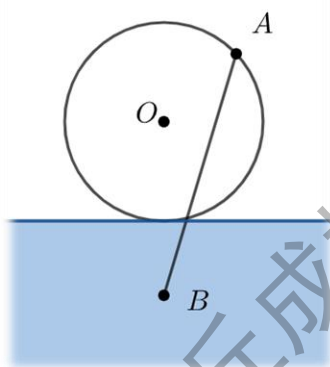


Figure 4-4 (a): Stretching phase

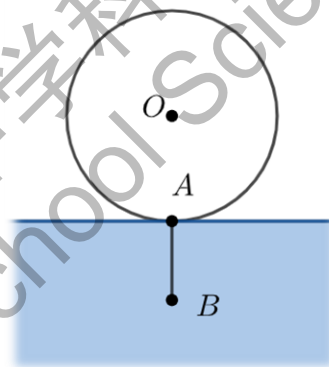


Figure 4-4 (b): Relaxing phase

It is indisputable that there are some differences between the cooling cycle of the prototype and that envisioned by the theoretical model. Firstly, the rubber bands only partly move between the hot and cold reservoirs with part of them remaining in the liquid all the time. Also, in reality, the conduction of heat can't be perfectly instant. Therefore, the coefficient of the real machine might be largely affected.

Before testing the prototype, we filled the container with 100ml of non-volatile oil and put it in an air-conditioned room overnight to make sure that it reaches ambient temperature. The temperature of the oil in the machine is originally at 26.7°C. In this experiment, we used 8 strands of rubber bands of the same type as those used in the previous isothermal stretching experiment. Their original length is 6cm and was stretched to a maximum length of 12cm in each cycle. When the motor was turned on, the temperature keeps dropping until it stabilized at 26.0°C about three minutes later. After the motor was turned off, we measured the temperature again and found it rose back to its original temperature.

V. Conclusion and Outlook

Through reading previous studies about the properties of rubber, we have learned various models about the mechanical properties of rubber bands including Hooke's Law and the more accurate MR model, but none of them takes the thermodynamic effect into account. Considering the microscopic structure of

rubber, we know that the coefficients in these models are related to temperature and rubber bands can be therefore used as the working medium of heat engines. With this idea, we started the research with the aim of finding the potential application of rubber in refrigeration to replace traditional Freon.

First, we conducted the experiment on the stretching process of rubber bands at different temperatures. Through the measured data, we've evaluated and verified the validity of MR model during isothermal stretching with maximum strain 100%. We've also tested the performance of the model we proposed about the tension change of elastomer in response to the increase of temperature, and this model was proved to be effective above 50% Strain while its performance was rather poor in lower strain energy (Appendix 2).

Next, using previous conclusion, we used the Maxwell relation to calculate the entropy change of the rubber band during stretching process and compared this result to the Gaussian model, where the result has shown that the Gaussian had extremely high performance when the strain is below 100%, but gradually lose its validity in higher strain region. We then compare with the result of total energy change predicted by MR model and Gaussian statistical model, and we were surprised to find that the ratio of rubber band heat gain to Strain energy change almost doesn't change in the stretching process. Based on this, we developed a more comprehensive model considering both the stretch state and temperature.

We also did other experiments in complementary to the previous one to study the behaviors of rubber bands in continuous stretching and contraction including hysteresis and fatigue, which are included in the Appendix 3~5.

Finally, we constructed thermodynamic cycle of a refrigerator based on rubber bands. To verify our idea, we designed and created a prototype machine, which caused a measurable temperature change 0.7°C .

Although our research gives some valuable results, there are still many aspects in which this topic can be further studied.

1. In this paper, we only studied rubber bands' response to temperature change in their stretching and contraction. However, rubber can also be twisted or compressed under external forces. Further studies can be done on the thermodynamic properties of rubber under other types of deformations.
2. So far, the scope of our research is limited to only one type of rubber band. To give a more general result, we can repeat our experiment on other types of rubber or other materials with similar microscopic structures.
3. Although our prototype machine shows measurable refrigeration, there are still many flaws in the mechanical design, and it is far from being capable for real-world applications. We hope that with better material and more considerations in the design, the performance of such a refrigerator can be improved.

VI. Bibliography

1. John Gough, "A description of a property of Caoutchouc." Memoirs of the Literary and Philosophical Society of Manchester, 2nd series, 1805.
2. Theodore A. Brzinski and Karen E. Daniels "Stretching Rubber, Stretching Minds: a polymer physics lab for teaching entropy" Department of Physics, NC State University
3. L. R. G. Treloar, "The Physics of Rubber Elasticity." Clarendon Press, Oxford, third edition, 1975
4. Qian, Suxin, et al. "A review of elastocaloric cooling: Materials, cycles and system integrations." International journal of refrigeration 64 (2016): 1-19.
5. Wang, Run, et al. "Torsional refrigeration by twisted, coiled, and supercoiled fibers." *Science* 366.6462 (2019): 216-221.
6. RUN WANG et.al, "The physics of Rubber Elasticity." CLARENDON PRESS OXFORD, Third Edition, 1975
7. M. Mooney, "A Theory of Large Elastic Deformation." Journal of Applied Physics 11, 1940
8. Marcy C. Boyce* and Ellen M. Arruda *, FLory: A Review." Department of Mechanical Engineering Center for Materials Science and Engineering Massachusetts Institute of Technology Cambridge, July 2000
9. David Roundy and Michael Rogers, "Exploring the thermodynamics of a rubber band." Am. J. Phys. 81 (1), January 2013
10. Jearl Walker, "Fundamentals of Physics." 14th Edition, 2005
11. Giancoli, Douglas C. Physics for scientists & engineers with modern physics. Pearson, 2014.
12. Mott, P. H., and C. M. Roland. "Limits to Poisson's ratio in isotropic materials." Physical review B 80.13 (2009): 132104. Mark W. Tibbitt, "Ideal polymer chains." ETH Zurich, 26 February 2019
13. Azadi, Somaye, et al. "Natural rubber identification and characterization in *Euphorbia macroclada*." Physiology and Molecular Biology of Plants 26.10 (2020): 2047-2052. Gou
14. Michiko Tazaki and Terutake Hooma, "On the Gough-Joule Effect of Rubber." October 1, 1985
15. R. L. Anthony, R. H. Caston, and Eugene Guth, "Equations of state for natural and synthetic rubber-like materials. Unaccelerated natural soft rubber*." Department of physics, university of Notre Dame, Indiana, first edition, 1943

VII. Thanks

Many people have lent a hand to us in our investigation and our work would never be done without their help. First, we would like to thank our Physics teacher Mr. Han Chaoqun. Much of our knowledge in Thermodynamics come from his industrious teaching and he provides lots of advice in the design of the experiment. Next, we want to thank Prof. Wang Sihui and Dr. Xiao Lintao, our external instructors. Their rigorous attitude helped us to formalize our writing and, when we were stuck in the theory part, they always guided us through the obstacles. Finally, we would like to thank Qu Renjie's father. He allowed us to use his professional photographic equipment and gave us instructions on its usage, which makes our data collection possible.

In the research process, all three members of our team collaborated close with each other from the procurement of experimental apparatus to the final format of the essay, trying hard to thoroughly investigate any detail in this topic and overcoming all the difficulties especially when our experiments failed. Qu Renjie contributed the most in the theory part and he first had the idea of connecting thermodynamics to MR model. He is also in charge of the process of experimental data. Dai Haochen designed all the experiments including the isothermal stretch and the refrigerator prototype. Li Yuchen is mainly responsible for the collection and sorting of the previous papers in this area and he provided some ideas for the design of the refrigerator.

VIII. Team Member's Information

Name: Dai Haochen

Gender: Male

School: Shanghai Pinghe School

Grade: Senior

Introduction: Enthusiastic in Physics and Engineering, is the president of Physics club and captain of robotic team of Shanghai Pinghe School.

Awards: 2021 British Physics Olympiad Top Gold, 2022 Physics Bowl D2 Silver

Name: Li Yuchen

Gender: Male

School: Shanghai Pinghe School

Grade: Senior

Introduction: Experienced in academic writing in science subjects, a lover of Physics, Environmental Science, and Sports

Awards: 2021 British Physics Olympiad Silver, 2022 Physics Bowl D2 Gold

Name: Qu Renjie

Gender: Male

School: Shanghai Pinghe School

Grade: Junior

Introduction: Proficient in using Python and other programming languages, good at mathematical deduction of Physics equations, is the president of Maths club and vice president of Physics club of Shanghai Pinghe School

Awards: 2021 British Physics Olympiad Gold, 2022 Physics Bowl D2 Silver

IX. Experimental location and time

7/11: 小组讨论, 确定题目 (磁流体和橡皮热力学), 最终决定橡皮筋热力学研究

7/17: 开始文献阅读, 小组讨论橡皮筋的应用 (制冷机)

7/23: 小组讨论, 开始筹备实验, 计划使用指针式弹簧测力计测量橡皮筋拉力, 开始采购器材: 包括但不限于航模橡皮筋, 亚克力管, 手持式电子温度计, 红外温度计, 橡胶塞, 自攻丝铁钩, 指针式弹簧测力计

8/2: 在戴同学家中进行第一次橡皮筋等温拉伸实验, 实验人员为戴同学和瞿同学

8/3: 实验没有得出任何结论: 指针式弹簧测力计的精度不足, 随机错误严重影响实验结果

8/4: 对前日实验做复盘, 写新的实验计划, 并对现有文献阅读得到的理论进行第一次总结: 不可压缩性, Gaussian model, MR model, Maxwell Relation, Hysteresis

8/13: 在戴同学家中尝试使用厨房电子秤间接测量拉力, 精度满足实验要求, 处理数据中发现数据与 MR model 符合较好, 因此将其作为理论基础

8/17: 在戴同学家中对之前在文献中发现的 Hysteresis 现象和橡皮筋的疲劳进行实验验证

8/23: 制冷机 CAD 设计及材料采购: 定制 3D 打印件, 激光切割亚克力板, 紧固件, 铝柱, 电机, 开关电源, 电机控制器, 同步带, 热熔胶

8/27: 制冷机的组装及实验验证, 实现了可测量的温度下降

X. Appendix

Appendix 1: Explanation and derivation of Gaussian Model

In the following paragraphs, with the limited materials given by Treloar in his book³, a complete relatively rigorous proof of the Gaussian entropy model in statistical thermodynamics view.

First of all, the general reason of the change in Boltzmann Entropy is basically because of the originally randomly oriented polymers become randomly oriented after stretch. Therefore, a seemingly reasonable way to approach the actual expression of Entropy change is to consider the change of entropy for each distinctive polymer, then sum up them through treatment of statistical Method.

For each single isolate long chain polymer, it could be roughly modeled as numerous chemical bonds jointed together from “head to tails” with every bond-link orientated randomly according to the assumption that we made. As a result, most of the long chain molecule will eventually form a curled-up 3D spatial structure, and its unfolding length will be much longer than its Relax state length.

Under this condition, according to the definition of Boltzmann Entropy, we can express the entropy by the probability density $P(x, y, z)$ with respect to state number of the polymer:

$$S = k \ln(P(x, y, z) dV \cdot \Sigma \Omega)$$

$$P(x, y, z) dx dy dz = \frac{\Omega(x, y, z)}{\Sigma \Omega}$$

Ω the microstate number, $P(x, y, z)$ the probability density

In order to further deduce the expression for the probability density, shall first consider the simpler expression of it in 1-D case. For the 1-D polymer model, each of its bonds has only two choices of orientation. Thus, for a polymer of length N , the sum of the number of possible states of all its lengths $\Sigma \Omega = 2^n$. Therefore, the probability density would be the following part.

$$P(x_1) = \frac{\Omega(x_1)}{\Sigma \Omega} = \frac{n!}{n_+! (n - n_+)! \cdot 2^n}, \text{ where } n_+ = \frac{n + n_1}{2} \text{ and } n_1 = \frac{x_1}{l}$$

Then, according to Sterling's Law and Taylor expansion, we could further deduce the simplified form of the probability density in 1-D cases.

$$\ln(P(x_1)) = n(\ln(n) - 1) - n_+(\ln(n_+) - 1) - (n - n_+)[\ln(n - n_+) - 1] - n \ln 2$$

$$LHS = \left(\frac{n + \frac{x_1}{l}}{2}\right) \left(\ln \frac{n}{n + \frac{x_1}{l}}\right) + \left(\frac{n - \frac{x_1}{l}}{2}\right) \left(\ln \frac{n}{n - \frac{x_1}{l}}\right)$$

$$\ln(P(x_1)) \approx -\frac{x^2}{2nl^2} \quad \text{this is second order term, } \therefore P(x_1) \approx a \exp\left(-\frac{x^2}{2nl^2}\right)$$

By considering the constant terms we neglected when using the Sterling's law and normalizing the discrete distribution probability, the continuous probability density distribution function for 1-D condition could be derived:

$$P(x) = \left(\frac{1}{2\pi nl^2}\right)^{\frac{1}{2}} \exp\left(-\frac{x^2}{2nl^2}\right)$$

Hence, we can conclude that this distribution of Probability satisfies the traditional Gaussian distribution when the links number reaches a certain value. As a result, it is easy by using Boltzmann Superposition principle to determine the 3-D distribution and entropy it since the polymers probability density satisfies Gaussian distribution in 1-D cases:

$$P(x, y, z)dV = P_{1D}(x)P_{1D}(y)P_{1D}(z)dx dy dz$$

$$S(x, y, z) = k \ln \left(P(x, y, z)dV \cdot \prod_{i=x,y,z} \Omega_{i \text{ total}} \right), \text{ where the } \pi \text{ part is constant}$$

Furthermore, due to the special form that the entropy function has, we could determine the expression of entropy for single polymer that consider the distance r between two terminals as the only variable:

$$\because l_x^2 + l_y^2 + l_z^2 = l_{3D}^2, \therefore l_x^2 = l_y^2 = l_z^2 = \frac{1}{3} l_{3D}^2$$

$$S(r) = k \ln \left(\left(\frac{1}{2\pi nl_i^2}\right)^{\frac{3}{2}} \exp\left(-\frac{x^2 + y^2 + z^2}{2nl_i^2}\right) dV \cdot \prod_{i=x,y,z} \Omega_{i \text{ total}} \right) = -\frac{3kr^2}{2nl_{3D}^2} + C$$

$$\text{where } \overline{l_{3D}^2} = nl_{3D}^2 \text{ is the RMS value of Bond length, } r^2 = x^2 + y^2 + z^2$$

$$C = k \ln \left(\left(\frac{3}{2\pi nl_{3D}^2}\right)^{\frac{3}{2}} dV \cdot \prod_{i=x,y,z} \Omega_{i \text{ total}} \right) \text{ is constant}$$

On the base of single polymer's expression and several assumptions that we've mentioned in the main body parts, the total entropy of the rubber band equals to the statistical sum of all the entropy of every polymer, and the (x, y, z) after stretched should satisfy the following equation

$$(x, y, z) = (\lambda_x x, \lambda_y y, \lambda_z z), \quad r' = \lambda r$$

where $\lambda_x \lambda_y \lambda_z$ are the stretch of three orthogonal principle direction

$$\therefore \Delta S = -\frac{3k}{2nl_{3D}^2} \Delta(r^2) = -\frac{3k}{2nl_{3D}^2} \Delta(x^2 + y^2 + z^2) = -\frac{3k}{2nl_{3D}^2} \left(\sum_{i=x,y,z} i^2 (\lambda_i^2 - 1) \right)$$

Considering $\lambda_1 \lambda_2 \lambda_3$ work as three parameters, then:

$$\Delta S_{\text{total per Unit Volume}} = -\frac{3k}{2nl_{3D}^2} \left(\sum_{i=x,y,z} \left(\sum i^2 \right) (\lambda_i^2 - 1) \right)$$

$$\sum x^2 = \sum y^2 = \sum z^2 = \frac{1}{3} \sum r^2 = \frac{N}{3} \overline{l_{3D}^2} \quad \text{where } N \text{ is the Number density of polymers}$$

Therefore, the final expression of Gaussian model could be simplified into the following form:

$$\Delta S_{total \text{ per Unit Volume}} = -\frac{1}{2}Nk(\lambda_1^2 + \lambda_2^2 + \lambda_3^2 - 3)$$

$$\text{where } I_1 = \lambda_1^2 + \lambda_2^2 + \lambda_3^2$$

The gaussian model of entropy firstly proved that the entropy isn't a function relate to temperature. It is easy to see that the final strain energy density function derived from the Gaussian model of thermodynamic statistics is very similar in form to the general form of the MR model. On the basis of this theory, scientists have invented MR model, Yeoh's model and other theoretical models similar to the above form in order to better fit the Large Strain (Non-Gaussian Region) and the actual change of Internal Energy during stretching.

Appendix 2: Tension change in response to temperature increase

Based on the temperature-stretch function that we proposed previously, compared with that by Flory⁸ and Erman^{*8}, we discovered that both of two terms in the Strain energy model given by Flory both has absolute temperature as its multiplication coefficients. Besides, we shall find that the Gaussian Entropy model also has the temperature as the main coefficient. Therefore, we could assume that the coefficients in the MR model should be proportional to the temperature as well as the tension:

$$W_{MN} = T(C_{10unit}(I_1 - 3) + C_{01unit}(I_2 - 3)), \quad \tau = 2S_0T \left(C_{10unit} + C_{01unit} \frac{1}{\lambda} \right) \left(\lambda - \frac{1}{\lambda^2} \right) \dots \dots (5)$$

With the equation we proposed, in the following paragraphs, we would further quantitatively analyzed the tension-temperature relationship during rubber band stretching, and the performance of the proportional model that we gave would also be evaluated by the data we gained from the former experiments which we chose to immerse the rubber band in the water of different temperatures contained in the acrylic tube for maintained the temperature unchanged. In addition, to ensure that the tensions under the same strain d not suffer from the random errors of the digital scale due to the response time and the minimum corresponding threshold, we choose to use the tension data under the corresponding strain given by the simulated MR model train (Since we have previously demonstrated the validity of the MR model in the interval from 10°C to 67.2°C, this method of pre-processing data is considered reasonable here) as raw data for this section.

Finally, we fitted the MR model of the rubber band at five temperature intervals of 67.2°C, 49.6°C, 40.1°C, 29.9°C, and 8.5°C ($\pm 1^\circ\text{C}$) through 163 data points, and selected the data at four strains of 20%, 50%, 80%, and 100% to investigate the relationship between the tension and temperature. We fitted the relationship between tension and temperature by the positive proportional function with lost function LMSE, and assisted with the linear function fit to evaluate the performance of the above proportional relationship and to conduct further analysis.

*8 P.J. Flory and B. Erman, *Macromolecules*, 15, 800, (1982). The model has the form of:

$$W_{FE} = W_{ph} + W_c, W_f = 12\xi kT \left(\sum_i \lambda_i^2 - 3 \right), W_c = \frac{1}{2} NkT \sum_i [B_i + D_i + \ln(B_i - 1) + \ln(D_i - 1)]$$

$$\tau_{MN} \propto T, \tau = 2S_0T \left(C_{10unit} + C_{01unit} \frac{1}{\lambda} \right) \left(\lambda - \frac{1}{\lambda^2} \right) \quad \text{Proportional fit function}$$

$$\tau_{MN} \propto (\alpha T + \beta)_l \quad \text{linear fit function (for Comparison)}$$

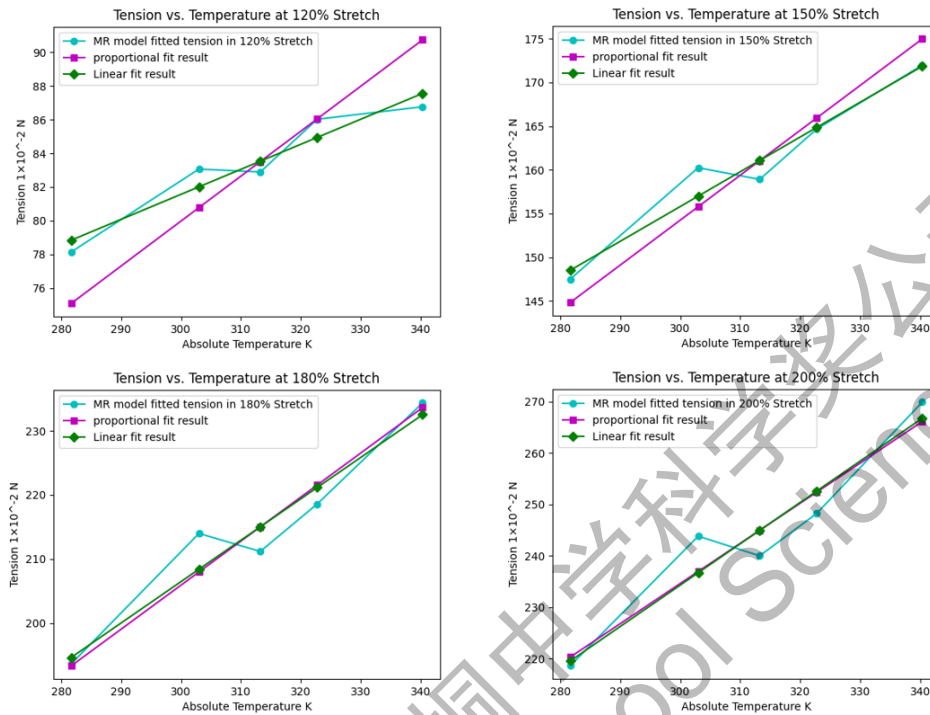


Figure 3-5~8: Tension (MR model fit) vs. Temperature graph at 120%, 150%, 180%, 200% Stretch respectively

Apparently, according to the blue broken lines in the above figures, we could find that the tensions corresponding to 40.1°C and 29.9°C in the above graph do not correspond to the positive tension-temperature correlation we predicted. Besides, even if we consider the possibility of a negative correlation between tension and temperature in the low-temperature interval found in the validated MR model, the strain value of such a negative correlation doesn't satisfy the condition that we verified in the above experiments, and by Anthony et.al in 1942¹⁹. However, since each of the two sets of data singled out satisfies Gough-Joule as a whole relative to the other temperature data, we took both sets of data into account in the actual proportional fit latter.

In general, we shall find out that the pre-processed tension vs temperature data overall follows roughly the same trend as our proposed positive scale model. Especially, in the region above 50% strain, the proportional fit has a very high simulation accuracy for the tension temperature data we obtained, and such correlation coefficients increases as the strain increases (the correlation increases from 0.9318 at 50% Strain to 0.9601 at 100% Strain.) However, below 50%, the proportional fit is much less effective than above 50% and cannot accurately predict the relationship between tension and temperature. (the correlation of the proportional model is only 0.5781 at 20% Strain).

In general, the proportional function we predicted before can predict the temperature dependence of the tension of the rubber band. Its performance is especially good in the high strain region while its performance in the low strain region is relatively poor.

Appendix 3: Fatigue effect

When discussing the mechanics of elastomer, the fatigue effect is an unneglectable phenomenon that should be addressed when analyzing repetitive and a large number of cycles. In the real world, fatigue might cause cracks inside the rubber material resulting in fracture of the elastomer, or it might cause the stress for a specific strain to keep decreasing along the repetition of the stretching process, which would be discussed later.

In general, various factors would affect the fatigue effect for an elastomer material such as the surrounding temperature, fatigue threshold, atmosphere environment, etc. In 1964, J.R. Beatty¹⁵ investigated the influences addressed on fatigue effect by surrounding temperature and maximum strain. The result showed that from 0 to 100 Celsius degrees under strain cycle 0-175%, the fatigue life of NR fibers only decreased by a factor of four while the original life cycle is 10^5 times. Similar results obtained by G. M. Bartenev et.al¹⁶, we could roughly conclude that: for the small number of stretching cycles that we conducted, the surrounding temperature won't largely influence the fatigue effect for the NR band, and the maximum strain of 200% is far less than the fatigue threshold of NR bands.

Furthermore, Liu Ji-yuan and Lie Xiao-dong used the kind of rubber band that we used in our experiment for the material fatigue test, and the result showed that the tension on the rubber band at fixed strain has an approximately linear relationship with the time of complete stretching-constrain cycle within the Maximum 2500 cycle numbers. Therefore, a preliminary experiment could be conducted, and a **segmentation linear-form compensation function** was deduced to correct the errors of data of tension caused by the Fatigue effect in later experiments.

Appendix 4: Preliminary experiment and the compensation function

In this preliminary experiment, we keep all the controlled variables (such as elastomer materials, and 0% strain length) aligned with the controlled variables of the later experiment. The purpose of this is to allow the resulting compensation function to be used directly in the subsequent processing of the experimental data

Original length l_0	Maximum Strain e	Room Temperature	Total cycle
18cm	88.9%	27.7°C	6

Table 2-1: Controlled variables for preliminary fatigue effect experiment

Since the Hysteresis fatigue of a single experiment is small and easily covered by the Random error of the measuring instrument, therefore, the values obtained from the first stretch and the sixth stretch were chosen for this experiment to compare and yield the coefficient of the compensation function with the following form:

$$\Delta\tau_{attenuate} = N\Delta\tau_{i,av} \text{ when } e_i \leq e < e_{i+1}, 'N' \text{ number of complete stretching process (6)}$$

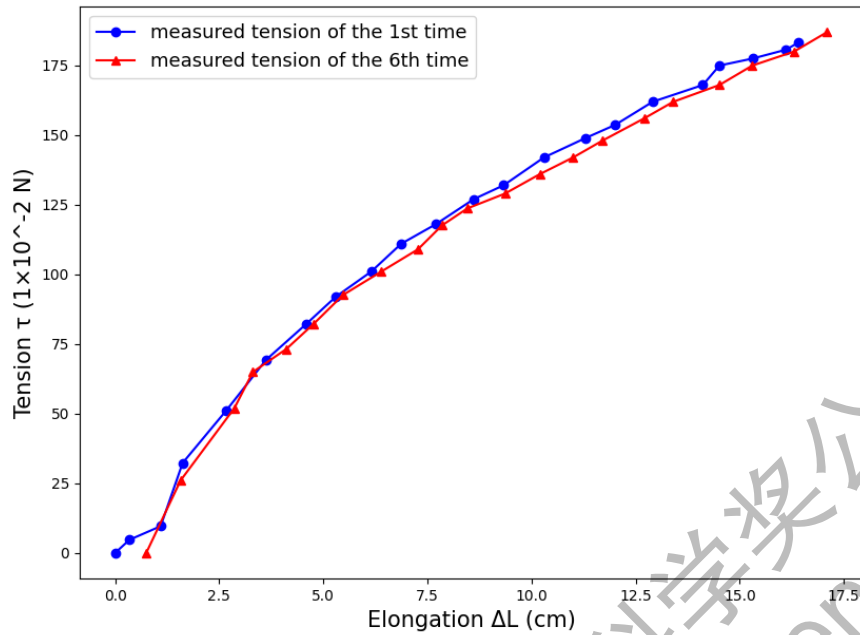


Figure 2-1: Comparison of Tension vs. Elongation graph for the 1st and 6th stretching. The Red one stands for the 1st time while the blue stand for the 6th.

According to the data, we shall find that at low strain, the tension of the rubber band still behaves very randomly with length. However, still, the effect of fatigue remained obvious even in low strain region: from the first stretch to the sixth stretch, the maximum elongation that has zero tensile strength in the Rubber band increases monotonically (from 0.00cm-0.20cm-0.76cm-0.88cm-1.03cm-1.44cm) with the increase of the number of stretches.

Therefore, after verified the validity throughout the whole process of stretching, through Interpolation, we could find out that the tension decay caused by Fatigue is presented as two more stable values in the Elongation interval of 2cm~6cm and 6cm~16cm respectively (i.e. the tension decay caused by fatigue can be approximated as a constant function with different ends in the two intervals respectively.) At this point, by subtracting the integral of tension within the corresponding interval and dividing the integrated value by the length of the interval, the average damping value of tension, also the segmented coefficient of the linear compensation function, could be determined:

$$\tau_{large} \approx -3.6 \times 10^{-2} N, \quad \tau_{small} \approx -2 \times 10^{-2} N$$

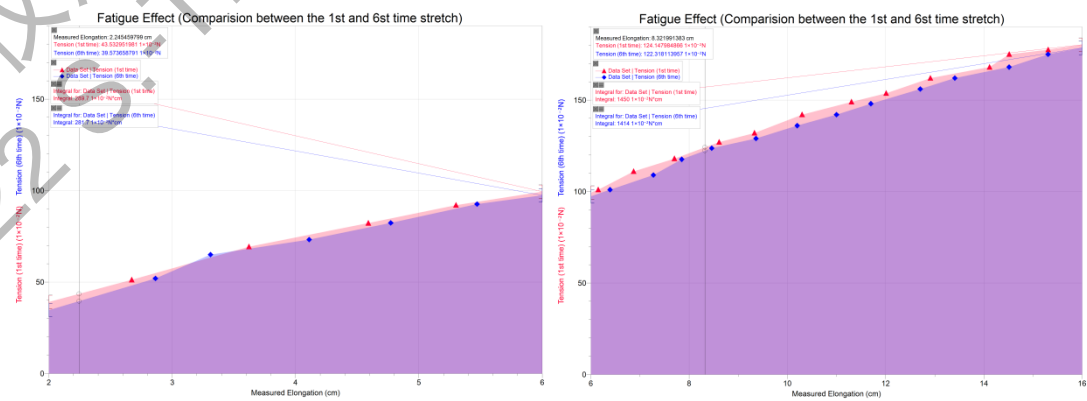


Figure 2-2&3: The difference in integral of the tension for two times within different strain intervals

Therefore, we could calculate the average fatigue of tension for each time in the interval 6cm~16cm and 2cm~6cm respectively:

$$\langle \tau_{small} \rangle \approx -0.4 \times 10^{-2} N, \quad \langle \tau_{large} \rangle \approx 0.712 \times 10^{-2} N$$

To smooth the transition of the average damping tension between two different intervals, two buffer zone was constructed with the form of a linear function based on the former compensation function:

Interval (cm)	0~2cm	2cm~5cm	5cm~7cm	7cm~16cm
$\tau_{comp}(\Delta l, N)$ (1×10^{-2} N)	$N \times 0.2\Delta l$	$N \times 0.4$	$N \times (0.156\Delta l - 0.38)$	$N \times (0.712)$

Table 2-2: Improved compensation function with the set-up of the buffer zone. ' Δl ' and ' N ' stand for the elongation length and number of cycles respectively.

Appendix 5: Hysteresis

The isothermal stretching experiment only measured the tension in the stretching process of the rubber band. However, to create a complete cycle for a heat engine, the rubber band needs to be stretched and released continuously. We realized that the rubber band may perform differently in stretching and contraction. Thus, we devised another experiment focused on one complete cycle. The apparatus and procedure of this experiment are the same as the stretching experiment. However, to evaluate the performance of larger strain to make further improvements on the rubber band refrigerator, we conducted this experiment with maximum strain at 200% to investigate the hysteresis effect and performance of the MR model at larger strain.

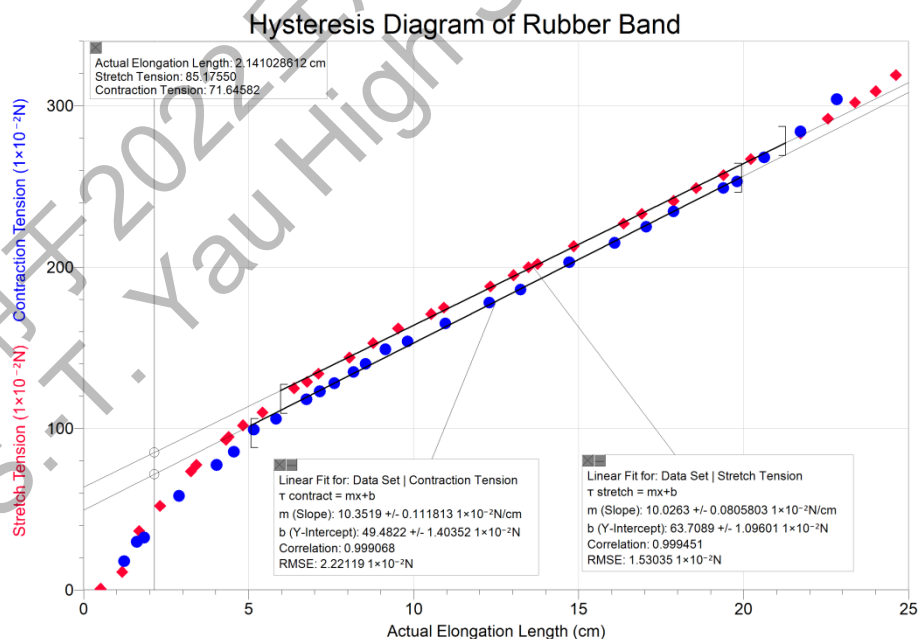


Figure 3-14: Tension versus elongation during stretching and contraction

In figure 3-14, the blue line that represents contraction can be divided into three phases. First, at very low elongations (0~5cm), the tension-elongation line curve has a decreasing steep slope. At an elongation

between 5~20cm (Strain between 40% and 170%), the trend is highly linear, which has a correlation coefficient over 0.999 for a linear fit. The value of tension is significantly lower than that of stretching at the same length, showing a hysteresis effect. For larger elongations, the slope increases again. The second major change in slope does not accord with the MR model. To fit this trend, inspired Yeoh Model⁸, we decided to take orders of I_1 terms in Rivlin's general representation⁸ of strain energy to create a better fit (Because usually a function of the type $ax^3 + bx^2 + cx$ can fit a curve that has a slope that first decrease than increase again with minimum computational complexity):

$$W_{improved} = C_{10}(I_1 - 3) + C_{01}(I_2 - 3) + C_{30}(I_1 - 3)^3$$

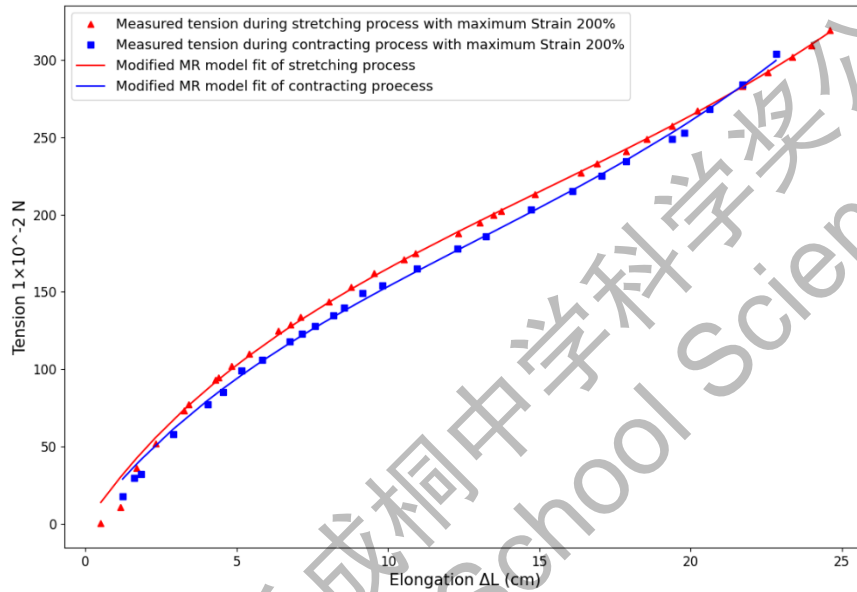


Figure 3-15: Hysteresis loop fit by Modified MR model

After deriving the theoretical thermodynamic cycle of a refrigerator based on the rubber band, we wanted to build a real machine to verify whether rubber can be the working medium for refrigeration. Given our limited budget, we didn't aim to build a machine that has real applications. Instead, we decided to use the accessible materials to design a prototype that is just capable of causing a measurable temperature decrease to demonstrate the cooling effect of our prototype.

报名学科	物理		参赛学生姓名	戴辰, 瞿任杰, 李宇晨	
论文题目	Exploring the Refrigeration ^{Thermodynamic} Effect of Rubber Band and Related properties Refrigerator Design				
指导教师信息					
姓名	韩超群		性别	男	
单位	上海平和双语学校		职称		
学历	研究生		专业	物理	
邮箱	hanchaoqun@shphschool.com		手机	13918060910	
身份类别	<input type="checkbox"/> 本校教师 <input type="checkbox"/> 科研机构专家 <input type="checkbox"/> 公益性校外教育机构老师 <input type="checkbox"/> 辅导机构老师 <input type="checkbox"/> 其他 (补充说明:) 提示: 须充分、据实填写, 可多选				
是否收费	<input checked="" type="checkbox"/> 无偿 <input type="checkbox"/> 有偿				
情况说明	您在研究报告的指导中具体参与哪些工作? <input type="checkbox"/> 选题指导 <input type="checkbox"/> 理论指导 <input checked="" type="checkbox"/> 实验指导 <input type="checkbox"/> 论文写作指导 <input type="checkbox"/> 其他 (补充说明:) (须充分、据实填写, 多选)				
信息确认	<div style="text-align: right;">  指导教师签字: 韩超群 (加盖单位公章) </div>				

2022 S.-T. Yau High School Science Awards